Synthesis of Tower-like ZnO Structures and Visible Photoluminescence Origins of Varied-Shaped ZnO Nanostructures

Feifei Wang,[†,‡] Li Cao,[†,‡] Anlian Pan,[†,‡] Ruibin Liu,[†,‡] Xiao Wang,[§] Xing Zhu,[§] Shiquan Wang,[†,‡] and Bingsuo Zou*[,†,‡]

Micro-Nano Technology Researches Center and State Key Lab of CBSC, Hunan University, Changsha 410082, China, and Institute of Physics, Chinese Academy of Sciences, Beijing 100080, China, and Department of Physics, Peking University, Beijing 100871, China

Received: October 31, 2006; In Final Form: January 17, 2007

Tower-like ZnO structures have been prepared by a simple carbon thermal reduction method and the possible growth mechanism of such structures was discussed. Comparing with microrods and nanowires, the photoluminescence images and spectra of tower-like ZnO were examined to understand the origins of their visible emissions, which is vital to future ultraviolet display devices. The visible photoluminescence locations of ZnO structures were studied by the near-field scanning optical microscopy. The experimental data indicate that the structure defects, surface impurities or dust, and adsorbed oxygen molecules can induce the visible emission of various ZnO nanostructures.

Introduction

ZnO as the II−VI semiconductor material has attracted more and more attention in the past few years because of its potential applications in many fields,[1−4] such as sensors, photocatalysis, field emission, and solar cells. Furthermore, ZnO also has important applications in ultraviolet lasers because of its large band gap (3.37 eV) and high exciton binding energy (60 meV). Because the size and morphology of ZnO have great effects on its properties and applications, people have prepared many different-shaped ZnO structures in order to fit different applications. So far, prismatic, belt-like, flower-like, tubular, tower-like, needle-like, and propeller-like ZnO have been reported using various physical and chemical techniques.[5−14] Though tower-like ZnO has been prepared by different techniques,[9−14] to our knowledge ZnO flowers made up of tower-like petals prepared by a simple carbon-thermal reduction method has not yet been reported.

As is well known, the surface recombination does not always quench the band-to-band recombination of ZnO, but it actually provides an undesirable trap of photoexcited carriers. Except for the ultraviolet emission, visible emission often occurs and even dominates in the photoluminescence of almost all ZnO nanostructures. Clearly understanding and decreasing the relaxation channel is important to the application of ZnO nanostructures as ultraviolet light emitters. Some efforts were tried to study the origins of visible emission in ZnO nanostructures. Vanheusden[15] reported that the green photoluminescence in ZnO is due to the recombination of electrons in single oxygen vacancies with photoexcited holes in the valence band. Hsu[16] found that both the band-edge and defect emission from aligned ZnO nanorods are strongly polarized and further indicated that deep-level transition occurred near the surface defects of the ZnO nanorods. Shalish[17] found that surface luminescence of ZnO nanowires is size-dependent and the surface luminescence increases as the wire radius decreases. Yet until now, no papers study systematically the origin and/or the spatial location of visible luminescence in ZnO nanostructures. Recent nanoscaled PL imaging techniques supply us the opportunities to look for the exact emission location in the ZnO nanostructures. Near-field scanning optical microscopy is one typical example of such techniques for obtaining subwavelength resolution (20−200 nm) with both the spectroscopy and spatial information by optical microscopy with far-field and near-field scanning. It has the ability to achieve topography and optical images with high spatial resolution and simultaneously measure the sample topography by controlling a submicrometer single-mode fiber probe close to the sample surface to collect the light from the sample.[18] To better understand the exact luminescence location, we used a commercial near-field scanning optical microscopy in collection mode to examine the photoluminescence in these nanostructures. In this paper, we studied the growth process and the origin of the visible emission of tower-like ZnO and compared the emission natures of tower-like ZnO with those of ZnO microrods and nanowires.

Experimental Section

Tower-like ZnO was prepared by a carbon-thermal reduction method as those usually used to prepare nanomaterials. Distinct from the conventional method of chemical vapor deposition, no catalysts were used in this experiment. Furthermore, neither carrier gas nor vacuum condition was needed. In our experiment, ZnO was synthesized in an electrical furnace with a horizontal quartz tube (35 mm in diameter, 100 cm in length). The source materials are pure ZnO and graphite powders. The two kinds of powders were mixed according to a certain ratio (1:1 by weight) and ground thoroughly in an agate mortar. Then the mixed powder was put into the center of a small special-shaped quartz tube (one side of the small tube is narrower than the other) in the horizontal quartz tube, and two pieces of clean silicon wafers as substrates to collect the sample were placed about 8−13 cm away from the powder. The small quartz tube was transferred into the center of the horizontal quartz tube of the furnace when the furnace temperature was 600 °C. Then the center temperature of the furnace was further raised to 1000 °C and maintained this temperature for an hour. After that,

* Author to whom should be addressed, E-mail: zoubs@aphy.iphy.ac.cn.
[†] Hunan University.
[‡] Chinese Academy of Sciences.
[§] Peking University.

10.1021/jp067151u CCC: $37.00
Published on Web 00/00/0000

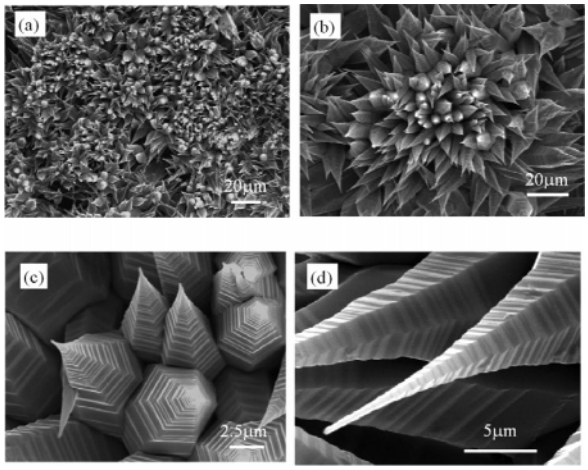

Figure 1. SEM images of the tower-like ZnO on silicon wafer in different magnification scales. (a) The low-magnification image; (b) the medium-magnification image; (c and d) the high-magnification images of the ZnO petals.

the furnace was shut down. When the furnace temperature was 650 °C, the small quartz tube was taken out from the furnace to cool down rapidly. After cooling down to room temperature, a white deposition layer (with samples A1 and A2 in the temperature region of about 770 and <740 °C, respectively) was found on the silicon wafers. Nanowires (sample B) were also formed on the wide side of this special-shaped tube, which is similar to the results reported by Cao[19] and Zou.[20]

The scanning electron microscope (SEM) images and the energy-dispersive X-ray spectrum (EDS) of the as-synthesized products were characterized by a scanning electron microscope (SEM, Hitachi, S-4200). The crystal structure was analyzed using an X-ray diffractometer (XRD) (Japan, Rigaku, D/MAX-2400) equipped with graphite-monochromatized Cu Kα radiation ($\lambda = 1.54178$ Å). The photoluminescence spectrum (PL) was taken on a PTI-C-700 fluorescence spectrometer. A CW He−Cd laser (50 mW, wavelength at 325 nm, IK 3552R-G) was used as the excitation source to measure the photoluminescence. The visible emission location of ZnO was investigated using a commercial near-field scanning optical microscope (NSOM) from RHK Technology using the He−Cd laser (325 nm) as the excitation source. A chromatic color CCD through an objective lens was used to collect the far-field topography and optical image. The lifetime decay profiles of ZnO were measured through the following setup. Laser pulses at 793 nm (~120 fs, 0.7 mJ, 1 kHz) were produced with a regenerative amplifier (Spitfire, Spectra Physics), which was seeded by a mode-locked Ti-sapphire laser (Tsunami, Spectra Physics). The produced pulses were frequency doubled in BBO to generate the second harmonic at 397 nm, which was then passed through another BBO crystal and generated a mixing signal at 266 nm with a highest output power of 15 mW. Then the pulse signal was perpendicularly excited onto the surface of the sample. The output fluorescence was focused into a monochromator and detected using a photon counting streak camera (Hamamatsu C2909). The time resolution is 30 ps, and the spectral resolution of the monochromator with 150 grooves/mm grating is 0.2 nm. All experiments were performed at room temperature.

Results and Discussion

The morphologies of as-prepared sample A1 were examined by SEM. Figure 1a is the general morphology of the as-synthesized ZnO on silicon wafer. Figure 1b shows the SEM image of a single ZnO flower. Figure 1c and d are the high-resolved SEM images of ZnO petals, and an obvious layer structure can be seen along the length direction of the petals. It can be seen from the SEM images that the silicon wafer was covered with flower-like ZnO in a large scale. The ZnO flower shown in Figure 1b resembles a blooming flower. A ZnO flower is composed of many tower-like ZnO petals, and each of the ZnO petals radiates from the center of the crystals to form a flower-like structure. The diameter of the tower decreases gradually from the bottom to the tip. At the bottom, the diameters are in the range of about 3−6 μm and the diameters at the tip are about several hundred nanometers. A hexagonal growth end plane and a growth tendency of layer by layer along the preferred growth direction can be identified clearly from the enlarged SEM images in Figure 1c and d. Furthermore, the high-resolved images reveal that these ZnO towers are sixfold symmetric, which indicate that they grow along the same direction.

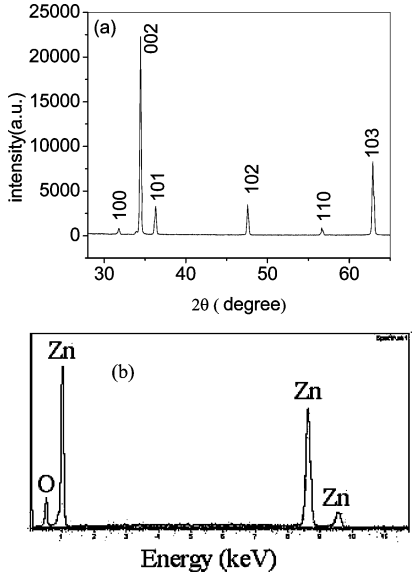

Figure 2. (a) XRD pattern and (b) EDS of the tower-like ZnO.

An XRD pattern was used to examine the crystal structure of the as-prepared ZnO. Figure 2a shows the XRD pattern of the tower-like ZnO. We can see that all of the diffraction peaks match with the standard data of hexagonal structural ZnO. The lattice constants ($a = 3.25$ Å, $c = 5.21$ Å) are in correspondence with the values in the standard card (JCPDS 36-1451). The stronger (002) diffraction peak indicates that (001) is the relatively preferred growth direction. An EDS associated with SEM shown in Figure 2b indicates that Zn and O are the elements of the sample, which is in agreement with the XRD analysis.

Why do such tower-like ZnO structures grow on the surface of the silicon wafer? In general, the vapor−liquid−solid (VLS)[21−24] process is a conventional growth mechanism to explain the catalyst-assisted nanostructural growth. The characteristic of the VLS growth is the existence of catalyst particles at the end of the 1D structure. In our experiment, no catalyst was evaporated on the silicon wafers, so the conventional VLS growth mechanism is not applied to this case and the possible growth process is the vapor−solid (VS) mechanism. Figure 3 shows the possible growth illustration of this special structure. Generally speaking, the zinc gase's concentration at an early stage has a great influence on the ZnO morphology.[25] During the synthesis, the zinc vapor generated by the carbonthermal reduction of ZnO was transported to the low-temperature region of the small asymmetrical tube. At the precursor position, the

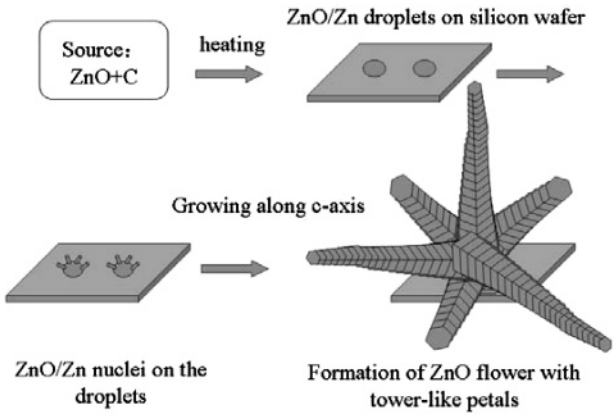

Figure 3. Growth illustration of a ZnO flower with tower-like petals.

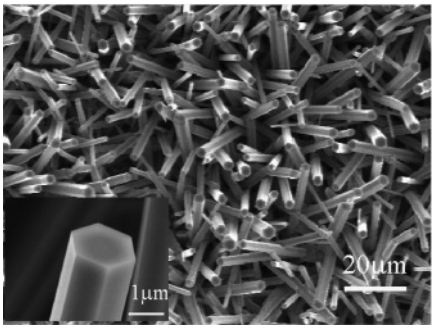

Figure 4. Morphology of ZnO on a low-temperature zone; the inset is the enlarged image of a single ZnO rod.

reductant graphite reacted with ZnO and oxygen and the Zn vapor in an oxygen-deficient environment produced rapidly. Then some of the Zn vapor reacted directly with oxygen, which resulted in the generation of ZnO/Zn vapor. In the low-temperature region, ZnO/Zn condensed on the silicon wafer as ZnO/Zn droplets. These droplets were energetically favored to adsorb zinc vapor and some of ZnO nucleated on the outer surfaces of these droplets. With increasing reaction time, zinc vapor fell on the nuclei continually. Those ZnO/Zn nuclei at an early stage acted as seeds for further growth of the petals along the preferred growth direction. Because the droplets at an early stage are much larger than nanometer scale, their depositions on the silicon surface probably behave like water on glass. After cooling down, the crystalline cross section of ZnO is large and then ZnO grows along different directions decided by the seeds. Because of a gradually decreasing supply of ZnO vapor,[14] tower-like structures were formed. At the same time, because the original growths of ZnO on the droplets were along different directions, the tower structures were also along different directions. Finally, tower-like ZnO petals grew radiatively to flower-like ZnO structure. We did a lot of experiments on this growth and found that the silicon wafer without Au particles, the high-temperature zone, and fast heating favor the tower-like structure.

It is reported by Gao et al.[12] that the local temperature and surface diffusion rate have great influence on the ZnO morphology. In this experiment, we observe that temperature, vapor flow, and the availability of the Zn−O vapor are important factors that affect the morphology of the as-prepared ZnO structure. Keep the other parameters constant and alter the position where the substrate was placed; the morphology of the ZnO may alter greatly. Figure 4 shows the sample prepared in the same condition as that of sample A1 except that the placed position was changed (in a low-temperature zone), which was about 2 cm away from the position where the A1 sample was placed. From Figure 4, we can see that the substrate was covered with hexagonal ZnO prisms (sample A2). Though the rods are not exactly perpendicular to the substrate, they do not assemble to a flower-like ZnO structure. Furthermore, the diameters of ZnO rods are smaller than the bottom diameters of the ZnO towers. The alternation of morphology and size may be caused by the decreasing of gas flow and temperature in the low-temperature zone, where less ZnO vapor and more oxygen can be supplied. So the excess Zn vapor, fast growth rate, and the gradually decreasing supply of ZnO vapor may be the cause of tower-structure formation.

The PL spectra of tower-like ZnO is shown in Figure 5a in which the lower and upper curves are the PL spectra before and after rinsing with ethanol, respectively. When excited by a laser beam at 325 nm from a He−Cd laser, the as-prepared ZnO shows a strong visible emission band at about 491 nm. Impurities and various intrinsic defects, such as the singly ionized oxygen vacancies and interstitial zinc atoms,[15,26−28] were usually assigned to be the origins of this visible emission band. The inset of Figure 5a shows the far-field PL image of the tower-like ZnO when it was excited by a He−Cd laser from the upward side of the sample, which shows a strong visible emission at the terrace edge of this structure. To understand the source of visible emission, we also measured the PL spectrum of this sample after rinsing with ethanol to remove the adsorbed extrinsic particle(s) on its surface. The adsorbed particles include molecules or small dust particles. After rinsing with ethanol, the relative intensity of visible emission decreased significantly and a UV emission from exciton-like near the band edge appeared in the PL spectrum. This indicates that the surface adsorption plays a significant role in the exciton relaxation after photoexcitation. We attribute the UV enhancement after rinsing partly to the adsorbed oxygen on the ZnO surface as that by the UV exposure.[29] The adsorbed oxygen creates a depletion region beneath the ZnO surface. When washed with ethanol, the adsorbed oxygen was reduced or excluded, and the depletion region was decreased. The increase of PL intensity may be concerned with the reduction of depletion region.[29] Furthermore, the dust on the ZnO surface also affects the luminescence and will be discussed in the next section. It was reported by Tong[30] that the tower-like ZnO structure has many edge dislocations parallel to the (0002) plane and the visible emission is associated with the surface/interface defects of this special structure. Though the UV emission was enhanced after rinsing, the visible emission still existed in the sample. The visible emission after rinsing may be concerned with the intrinsic structure of the tower-like structure. The tower ZnO structure contains high-density surface/interface defects like terrace and cusp, which might induce deep energy levels within the band gap and trap the free or photoexcited carriers from the inside. When the sample was excited by the laser, the generated carriers can recombine with the surface/interface states at these deep levels. The recombination of a trapped electron to the hole in the defect band leads to the visible emission.

For the perfect surface, the adsorbed particles also play their roles in the relaxation processes. The far-field PL image of a ZnO microrod with obvious impurities or dust on the surface was also obtained[31] by the above technique and shown in Figure 5b1. During the growth process or a later processing process, other intended impurities, such as MnO, Fe_2O_3, Al_2O_3, CuO, or S and so forth, may deposit on the surface of the ZnO nanostructures. It is not avoidable for the dust to adhere on the surface when the sample is exposed to the heating impurity or ambient air in the tube, and we can obviously see some

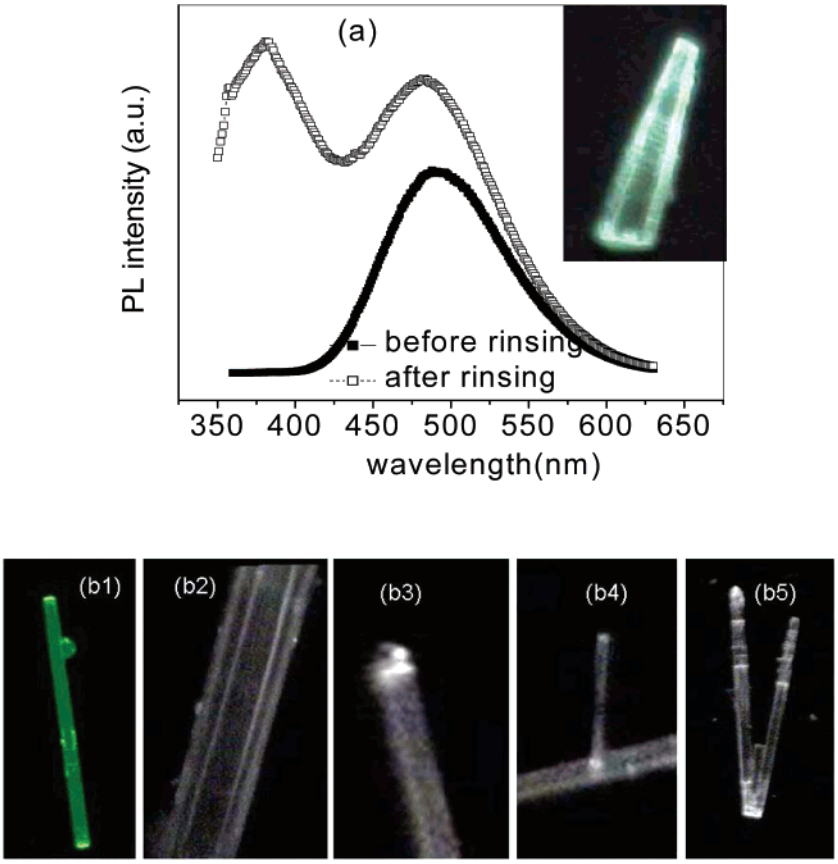

Figure 5. (a) PL spectra of tower-like ZnO before and after rinsing with ethanol, and the inset is the far-field PL image of this sample. (b) The far-field PL images of different ZnO structures.

impurities and dust on the surface of nanowires via microscopy, as shown in Figure 5b1. When rinsing the ZnO sample with deionized water to remove the impurities or dust on it, a phenomenon similar to that of tower-like ZnO rinsing with ethanol was found but the relative intensity of the UV is much smaller. Combining the PL spectrum (not shown in this paper) with the PL images in Figure 5b, we can see that the surface impurities or dust are also the source of visible emission. The dust−ZnO structure behaves as an extrinsic defect with a deep level, which traps the exciton to give a green emission. Moreover, it can be seen from the image that the brightness of the two end faces of the rod is much stronger than that in the middle part, which indicates the good waveguide behavior of this microrod.[31] The visible emission can also lead to a waveguide along the longitudinal direction and emitted at the end surface. This indicates that the emitted light on the surface can penetrate into the nanorod and then propagate through the longitudinal direction of a rod. To illustrate clearly the special location of the visible emission, we also gave the far-field enlarged PL images of the ZnO rod, the ZnO rod with obvious particles on its end plane, and branched ZnO structures as are shown in Figure 5b2, b3, b4, and b5. (Figure 5b2, b3, b4, and b5 were obtained by another near-field system and shown in black and white, though obvious green luminescence can be seen by the naked eyes.) It can be seen from Figure 5b2, b3, b4, and b5 that the visible emission were located obviously at the edge (arris) of the ZnO rod, the end surface especially being the location with obvious impurities, and the end surfaces of the branch.[31] Although these emissions can be saturated easily at a higher excitation power, their spatial distribution is vital to further applications. Understanding the emission location will help us design some devices in further applications; for example, the branched ZnO will be used in multipath emission devices.

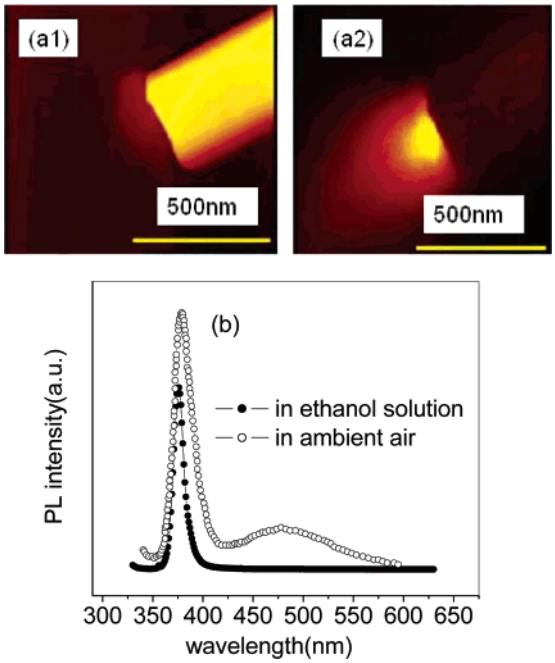

Figure 6. Near-field topography (a1) and PL image (a2) of the end of the ZnO nanowire. (b) The PL spectra of ZnO nanowires in ambient air and in ethanol solution.

Additionally, the near-field topography and PL image of the pure ZnO nanowires (sample B) with perfect crystallization are shown in Figure 6a. By comparing the near-field topography with PL images, we can see clearly that the PL was located on the end of a nanowire. The PL spectra of pure ZnO in clean ambient air and in ethanol solution were also measured and

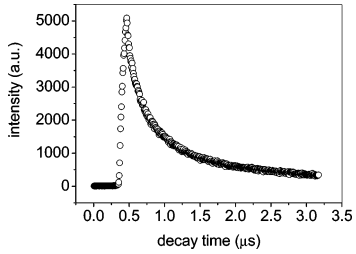

Figure 7. PL lifetime decay profile of the visible emission of ZnO.

shown in Figure 6b. In ambient air, the newly prepared ZnO nanowires show a strong UV emission band and a much weaker visible band, whereas the PL spectrum of the ZnO nanowires, dispersed immediately in ethanol after taking out from the tube furnace, only shows the UV band. This indicates that oxygen molecules adsorbed on the surface in ambient air participate in the visible emission, whereas in ethanol the ethanol molecule washes out the oxygen adsorbed on the ZnO surface. In ambient air, the electrons in ZnO will transfer from the bulk to the adsorbed oxygen and lead to the formation of a depletion layer,[32] and the depleted layer can decrease the radiative recombination of electrons and holes. It was reported by Jin[29] that after a period time of UV exposure, both the intensity of the UV emission and the visible emission was enhanced and they attributed the UV emission enhanced effect to the desorption of oxygen on the ZnO thin-film surface. The thermal treatment in hydrogen ambient could also lead to the desorption of oxygen on the surface of ZnO nanostructures and enhancing PL.[33,34] Comparing the PL spectra in ethanol and in ambient air, the effect of adsorbed oxygen on the photoluminescence of ZnO was observed. So the adsorbed oxygen on the surface of the ZnO crystal has great effects on its emission properties. For future luminescence applications, it is important to diminish the structural defects and adsorbed oxygen on the surface of ZnO nanostructures.

In the above discussion, we analyzed the visible luminescence of ZnO from the point of spatial emission location. We can see that structure defects, impurities, and adsorbed oxygen are the causes of visible emission of the ZnO structure. Figure 7 gives the decay time of trap-state recombination of ZnO nanostructures. It can be seen that the decay time of visible emission is close to one microsecond. At low pump fluence, because of the abundance trap states in these ZnO structures, the UV emission cannot be observed and visble emission is dominant. Compared to the UV emission, the population and radiative recombination process of the trap states is very slow. If the density of the trap states is not high, then they may be occupied soon after photoexcitation and then saturated. So, the UV emission in the nanosecond scale will become the main radiative recombination process and is easily seen even in imperfect ZnO nanostructures and under low pump fluence. Therefore, the lifetime of 1 μs may contain the propagation time of waveguiding light. Under high excitation, enough photogenerated carriers and the slow radiative recombination rate make the trap states easy to be saturated. The recombination process by the trap states may be inappreciable as compared to the UV emission, and the stimulated UV emission by exciton−exciton scattering can be seen under high excitation in the doped ZnO nanostructure.[20] Though the stimulated emission can be seen in imperfect ZnO, the threshold power of the imperfect sample is higher than that of the perfect sample, which may cause thermal damage in ZnO nanostructures.[20] So the trap states in the ZnO sample have great effects on both the spontaneous emission and the stimulated emission.

Above all, it was demonstrated by the experiments that structure defects, such as edge dislocations, impurities, and adsorbed oxygen, are three types of causes of visible luminescence in ZnO nanostructures. ZnO long time exposure to ambient indoor environments can reduce the UV PL intensity.[29] It is important to take measures to avoid surface contamination or passivation of the surface by coating with a protecting layer of silicon oxide or aluminum oxide for future applications in luminescence devices. Our results indicate that the ZnO towers and nanowires may be used for gas sensors by detecting their visible luminescence.

Conclusions

In summary, the tower-like ZnO was prepared by a carbon thermal reduction method. The possible growth mechanism was discussed. To explore the origin and location of visible emission, systematically PL and NSOM experiments of tower-like ZnO, ZnO microrods, and ZnO nanowires were carried out. It was observed that the visible PL spectrum of tower-like ZnO after rinsing is concerned with the defects of this special structure; surface impurities or dust are one source of visible emission in ZnO microrods, and adsorbed oxygen also affects the visible luminescence of ZnO nanowires besides the doping effect. So, the surface conditions are very important to the luminescence of ZnO structures and we can obtain the intrinsic exciton emission by changing their surface conditions.

Acknowledgment. We thank the financial supports of NSFC of China (Term no. 90606001 and 90406024), National 973 project (2002CB713802), project (grant No.705040) of MOE of China and 985 fund of HNU.

Note Added after ASAP Publication. This article was released ASAP on May 9, 2007. The authors' address line and footnotes regarding their affiliations has been revised. The corrected version was posted on May 16, 2007.

References and Notes

(1) Hara, K.; Horiguchi, T.; Kinoshita, T.; Sayama, K.; Sugihara, H.; Arakawa, H. *Sol. Energy Mater. Sol. Cells* **2000**, *64*, 115.

(2) Rodriguez, J. A.; Jirsak, T.; Dvorak, J.; Sambasivan, S.; Fischer, D. *J. Phys. Chem. B* **2000**, *104*, 319.

(3) Yumoto, H.; Inoue, T.; Li, S. J.; Sako, T.; Nishiyama, K. *Thin Solid Films* **1999**, *345*, 38.

(4) Liu, C.; Zapien, J. A.; Yao, Y.; Meng, X.; Lee, C. S.; Fan, S.; Lifshitz, Y.; Lee, S. T. *Adv. Mater.* **2003**, *15*, 838.

(5) Li, W. J.; Shi, E. W.; Zhong, W. Z.; Yin, Z. *J. Cryst. Growth* **1999**, *203*, 186.

(6) Gui, Z.; Liu, J.; Wang, Z. Z.; Song, L.; Hu, Y.; Fan, W. C.; Chen, D. Y. *J. Phys. Chem. B* **2005**, *109*, 1113.

(7) Yin, H. Y.; Xu, Z. D.; Wang, Q. S.; Bai, J. Y.; Bao, H. H. *Mater. Chem. Phys.* **2005**, *91*, 130.

(8) Pan, A. L.; Yu, R. C.; Xie, S. S.; Zhang, Z. B.; Jin, C. Q.; Zou, B. S. *J. Cryst. Growth* **2005**, *282*, 165.

(9) Wang, Z.; Qian, X. F.; Yin, J.; Zhu, Z. K. *Langmuir* **2004**, *20*, 3441.

(10) Zhang, B. P.; Binh, N. T.; Wakatsuki, K.; Usami, N.; Segawa, Y. *Appl. Phys. A* **2004**, *79*, 1711.

(11) Meng, X. Q.; Shen, D. Z.; Zhang, J. Y.; Zhao, D. X.; Dong, L.; Lu, Y. M.; Liu, Y. C.; Fan, X. W. *Nanotechnology* **2005**, *16*, 609

(12) Gao, P. X.; Wang, Z. L. *Appl. Phys. Lett.* **2004**, *84*, 2883.

(13) Umar, A.; Lee, S.; Im, Y. H.; Hahn, Y. B. *Nanotechnology* **2005**, *16*, 2462.

(14) Hu, P. A.; Liu, Y. Q.; Wang, X. B.; Fu, L.; Zhu, D. B. *Chem. Commun.* **2003**, *11*, 1304.

(15) Vanheusden, K.; Warren, W. L.; Seager, C. H.; Tallant, D. R.; Voigt, J. A.; Gnade, B. E. *J. Appl. Phys.* **1996**, *79*, 7983.

(16) Hsu, N. E.; Hung, W. K.; Chen, Y. F. *J. Appl. Phys.* **2004**, *96*, 4671.

(17) Shalish, I.; Temkin, H.; Narayanamurti, V. *Phys. Rev. B* **2004**, *69*, 245401.

(18) Ben-Ami, U.; Nagar, R.; Ben-Ami, N.; Scheuer, J.; Orenstein, M.; Eisenstein, G.; Lewis, A.; Kapon, E.; Reinhardt, F.; Ils, P.; Gustafsson, A. *Appl. Phys. Lett.* **1998**, *73*, 1619.

(19) Cao, L.; Zou, B. S.; Li, C. R.; Zhang, Z. B.; Xie, S. S.; Yang, G. Z. *Europhys. Lett.* **2004**, *68*, 740.

(20) Zou, B. S.; Liu, R. B.; Wang, F. F.; Pan, A. L.; Cao, L.; Wang Z. L. *J. Phys. Chem. B* **2006**, *110*, 12865.

(21) Morales, A. M.; Lieber, C. M. *Science* **1998**, *279*, 208.

(22) Wu, Y. Y.; Yang, P. D. *Chem. Mater.* **2000**, *12*, 605.

(23) Duan, X. F.; Lieber, C. M. *Adv. Mater.* **2000**, *12*, 298.

(24) Huang, M. H.; Mao, S.; Feick, H.; Yan, H. Q.; Wu, Y. Y.; Kind, H.; Weber, E.; Russo, R.; Yang, P. D. *Science* **2001**, *292*, 1897.

(25) Shen, G. Z.; Cho, J. H.; Lee C. J. *Chem. Phys. Lett.* **2005**, *401*, 414.

(26) Bylander, E. G. *J. Appl. Phys.* **1978**, *49*, 1188.

(27) Vanheusden, K.; Seager, C. H.; Warren, W. L.; Tallant, D. R.; Voigt, J. A. *Appl. Phys. Lett.* **1996**, *68*, 403.

(28) Kang, H. S.; Kang, J. S.; Kim, J. W.; Lee, S. Y. *J. Appl. Phys.* **2004**, *95*, 1246.

(29) Jin, C. M.; Tiwari, A.; Narayan, R. *Jpn. J. Appl. Phys.* **2005**, *98*, 083707.

(30) Tong, Y. H.; Liu, Y. C.; Shao, C. L.; Mu, R. X. *Appl. Phys. Lett.* **2006**, *88*, 123111.

(31) Cao, L.; Zou, B. S.; Pan, A. L.; Wu, Z. Y.; Zhang, Z. B.; Xie, S. S.; Liu, D.; Zhang, W. H.; Zhu, X. *Phys. Low-Dimens. Struct.* **2006**, *1*, 36.

(32) Lin, Y. H.; Wang, D. J.; Zhao, Q. D.; Li, Z. H.; Ma, Y. D.; Yang, M. *Nanotechnology* **2006**, *17*, 2110.

(33) Baik, S. J.; Jang, J. H.; Lee, C. H.; Cho, W. Y.; Lim, K. S. *Appl. Phys. Lett.* **1997**, *70*, 3516.

(34) Oh, B. Y.; Jeong, M. C.; Kim, D. S.; Lee, W.; Myoung, J. M. *J. Cryst. Growth* **2005**, *281*, 475.